Quantification of Protein Incorporated into Electrospun Polycaprolactone Tissue Engineering Scaffolds

Nicole E. Zander,*[†,‡] Joshua A. Orlicki,[†] Adam M. Rawlett,[†] and Thomas P. Beebe, Jr.[‡]

[†]U.S. Army Research Laboratory, Weapons and Materials Research Directorate, Aberdeen Proving Ground, Maryland 21005, United States

[‡]Department of Chemistry and Biochemistry, University of Delaware, Newark, Delaware 19716, United States

ABSTRACT: The surface modification of synthetic tissue engineering scaffolds is essential to improving their hydrophilicity and cellular compatibility. Plasma treatment is an effective way to increase the hydrophilicity of a surface, but the incorporation of biomolecules is also important to control cellular adhesion and differentiation, among many other outcomes. In this work, oriented polycaprolactone (PCL) electrospun fibers were modified by air-plasma treatment, followed by the covalent attachment of laminin. The amount of protein incorporated onto the fiber surface was controlled by varying the reaction time and the protein solution concentration. The protein concentration and coverage were quantified using X-ray photoelectron spectroscopy (XPS), solid-state ultraviolet–visible spectroscopy (UV–vis) and two fluorescence-based assays. XPS results showed a nearly linear increase in protein coverage with increasing protein soaking solution concentration until a monolayer was formed. Results from XPS and the NanoOrange fluorescence assay revealed multilayer protein coverage at protein solution concentrations between 25 and 50 μg/mL, whereas the UV–vis assay demonstrated multilayer coverage at lower protein solution concentrations. The effect of protein concentration on the neurite outgrowth of neuron-like PC12 cells was evaluated, and outgrowth rates were found to be positively correlated to increasing protein concentration.

KEYWORDS: electrospinning, nanofibers, nerve regeneration, protein quantification, protein coverage, XPS
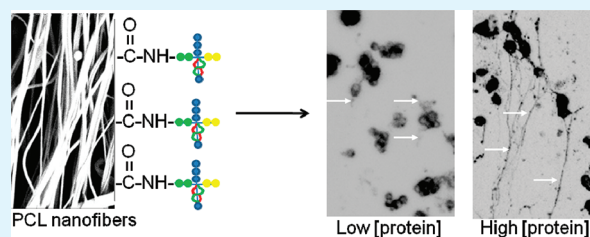
INTRODUCTION

The major function of a tissue engineering scaffold is to provide a three-dimensional environment to support and guide cellular adhesion, proliferation and differentiation, promoting the formation of complex tissue.[1,2] Scaffolds should be biocompatible, biodegradable, match the mechanical properties of the tissue with which it will interface, and maintain permeability to molecules needed by the cells. Scaffolds can be composed of natural, synthetic or modified-synthetic materials. Natural scaffolds have the obvious advantage of sharing mechanical, physical, and chemical properties of the tissues they are replacing, but their high cost is a limiting factor. Synthetic scaffolds are much more cost-efficient, and the mechanical and physical properties can often be tailored to the application.[3] The majority of synthetic polymers used to support tissue engineering possess the aforementioned scaffold characteristics but lack biorecognition sites such as proteins or growth factors to communicate with and direct cells. In addition, many polymers are fairly hydrophobic and allow for only limited adhesion and spreading of cells.[4,5] Thus, it is desirable to modify scaffolds to increase both the hydrophilicity and introduce surface active groups for protein attachment to improve the cellular compatibility, and hence modified-synthetic scaffolds are a good choice.

There is an array of techniques to modify scaffolds to increase the hydrophilicity and introduce active sites for the attachment of biomolecules, including plasma modification, wet chemical methods, surface graft polymerization, blending the synthetic polymer with a natural polymer, or the physical adsorption of proteins on the scaffold surface.[4,6–9] Of the aforementioned modification methods, techniques that introduce surface functional groups allowing for the covalent immobilization of biomolecules are favored as the molecules do not leach from the surface. The incorporation of biomolecules into synthetic scaffolds helps to mimic the chemical environment of the extracellular matrix (ECM). It is also necessary to mimic the physical structure and the mechanical properties of the ECM, as shown for many cell types including mesenchymal stem cells and neurons.[10–13]

Electrospinning is a technique that produces fibers of similar size scale to the fibrous components of some tissue types' ECM. Electrospinning is gaining much attention in the tissue engineering field due to the ease of scaffold formation and versatility of the technique. Fiber composition, diameter, alignment, and scaffold porosity can be tailored for the particular cell or tissue type.[14–18] Furthermore, the high surface area-to-volume ratio makes electrospun nanofibers attractive candidates for the surface modification techniques discussed

above, particularly protein immobilization.[3,19] Polycaprolactone (PCL) is an FDA-approved biomaterial, which has the desired properties of biocompatibility and biodegradability, along with good mechanical properties. It is one of the most common polymers used for nerve tissue engineering, along with polylactic acid (PLLA) and polyglycolic acid (PGA).[20] In a study by Sangsanoh et al., the viability of rat Schwann cells was found to be higher on PCL nanofibers in comparison to PLLA and polyhydroxybutyrate (PHB) nanofibers.[21] On the basis of the aforementioned study, and the relative cost of the materials, we decided to use PCL as our scaffold matrix for these studies.

The surface concentration of protein has been found to be an important factor in controlling cellular processes. Shi et al. discovered a strong positive correlation between cellular adhesion and fibronectin protein concentration for NIH 3T3 cells.[1] Straley et al. found that increasing the RGD peptide surface density increased both cell adhesion and neurite outgrowth of PC12 cells.[22] Dertinger et al. and Adams et al. found that the axons of neurons orient in the direction of increasing laminin concentration gradients.[23,24]

Although it is well-known that protein substrates are beneficial for tissue engineering, techniques to control protein concentration and a thorough study of protein quantification methods on electrospun fibers have been little examined. In this work, the ECM protein laminin was covalently immobilized on electrospun polycaprolactone (PCL) fibers. Surface and total functional group and protein coverage were examined using X-ray photoelectron spectroscopy (XPS), ultraviolet−visible spectroscopy (UV−vis), and immunofluorescence assays. In addition, the effect of protein concentration on neurite outgrowth for nerve regeneration scaffolds was explored using the neuron-like PC12 cell line.

■ MATERIALS AND METHODS

Materials. Polycaprolactone with an average molecular weight of 40 kDa was obtained from Polysciences, Inc. Anhydrous N,N-dimethylformamide (DMF), mouse laminin, rabbit antilaminin, paraformaldehyde, Tween 20, N-(3-Dimethylaminopropyl)-N'-ethylcarbondiimide (EDC), N-hydroxysuccinimide (NHS), 2-(N-morpholino)ethanesulfonic acid (MES), Triton X-100, and ninhydrin were obtained from Sigma-Aldrich. Dichloromethane, Dulbecco Modified Eagle's Medium (DMEM), RPMI 1640, calf serum, horse serum, trypsin-EDTA, phosphate buffered saline (PBS), nerve growth factor (NGF 7S) and CellTiter 96 AQueous Assay (MTS) were obtained from Fisher Scientific. Antibiotic/antimycotic was obtained from Cellgro (cat. 30−004-C1). NanoOrange, 5-(aminoacetamido) fluorescein, rhodamine phalloidin, and AlexaFluor 488 donkey antirabbit IgG were obtained from Invitrogen.

Fabrication of Electrospun Fibers. A 20 wt % solution of PCL was prepared by dissolving the polymer in a 50:50 (w/w) mixture of anhydrous DMF and dichloromethane with stirring at RT overnight. PCL fibers were electrospun using a custom-built apparatus consisting of a syringe pump (Aladdin AL-1000) and a rotating 2 in. width, 1 in. diameter mandrel. The mandrel was connected to a motor (Bodine NSH-12R) with a speed controller (Minarik Electric Company SH-14), allowing the mandrel to rotate between 0 and 5000 rpm. A 5-mL syringe was filled with polymer solution and fed through a 21G stainless steel needle at flow rates of 1−5 mL/h with an applied potential of 18.5 kV. The gap between the needle and the collector was fixed at 7 in. and the collector was set to an applied potential of −3 kV. Fibers were dried under vacuum at RT overnight before characterization and functionalization.

Electrospun Fiber Modification. Vacuum-dried PCL fibers were plasma treated in air using an inductively coupled radio frequency (RF) plasma cleaner (Harrick PDC-32-G) for 5 min at a RF power of 18 W to introduce carboxylic acid and other oxygen-containing

functionalities to the surface of the fibers. The mats were cut to fit into 24-well plates. Plasma-treated fibers were then immersed in a MES buffer containing of 5 mg/mL EDC and 5 mg/mL NHS for 1 h at RT.[25] Fiber mats were rinsed with MES buffer and incubated in a laminin solution at 4 °C for the specified time period. The protein solution was removed and the mats were washed in a 0.05% Tween 20 solution in PBS with gentle shaking for 30 min to remove physically absorbed protein. Mats were then washed thoroughly with PBS and sterilized overnight by immersing in a sterile solution of 2% antibiotic/antimycotic in PBS. Samples were kept sterile for cell culture studies or rinsed thoroughly with deionized water and dried for characterization.

Characterization of Scaffolds. The morphology of the fiber scaffolds was examined using a field-emission scanning electron microscope (Hitachi S-4700) in the secondary-electron mode, using a mixture of upper and lower detectors. An accelerating voltage of 0.6 kV was maintained in order to prevent surface damage to the substrate. Before observation, the samples were first coated with approximately 10 nm of gold using a sputter coater (Hummer XP Sputtering System, Anatech LTD). Several areas were imaged in order to examine the uniformity of the fiber diameters. Fiber diameters were measured using image analysis software (Image J v 1.34, National Institutes of Health).

The wettability of the surface was determined using a sessile drop contact angle system (First Ten Ångstroms) with an RS170 camera. The contact angles were measured and calculated using an automated fitting program (FTA32 v2.0). All reported contact angles are the average of $n = 5$ measurements each on 3 replicate fiber mat samples. Deionized water was used to test the contact angle of the fiber mats (Milli-Q filtration system).

Surface compositional analysis was performed using a Kratos Axis Ultra 165 X-ray photoelectron spectroscopy (XPS) system equipped with a hemispherical analyzer. Sampling areas of 1 mm × 0.5 mm were irradiated with a 100 W monochromatic Al $K\alpha$ (1486.7 eV) X-ray beam at a takeoff angle of 90°.The XPS chamber pressure was maintained between 1×10^{-9} and 1×10^{-10} Torr. Elemental high-resolution scans were conducted with a 20-eV pass energy for the C 1s, O 1s and N 1s core levels. A value of 284.6 eV for the methylene component of the C 1s spectrum was used as the calibration energy for the binding energy scale, and all other spectra were shifted by the corresponding amount. Data were processed using Casa XPS software v 2.3.5. All reported atomic percentages are the average of $n = 2$ measurements each on a minimum of 3 replicate fiber mat samples.

Functional Group and Protein Quantification. Total functional group concentration was examined using a Perkin-Elmer Lambda-950 UV−vis Spectrometer. The scan range was set between 300 and 800 nm, and the PMT response was fixed at 10 s with 4 nm resolution. The concentration of surface carboxylic acids on the fibers was determined using an assay with 5-(aminoacetamido) fluorescein. Unmodified PCL mats and unmodified and plasma-treated PCL mats reacted with EDC/NHS were soaked overnight in a 0.1-mM solution in PBS at RT with gentle shaking. Mats were thoroughly rinsed with PBS and water, and dried for analysis. The surface-equivalent carboxylic acid concentration per fiber mat mass was calculated from a standard 5-(aminoacetamido) fluorescein calibration curve, using a linear least-squares fit.

The surface-equivalent concentration of laminin protein was determined using a Ninhydrin assay, which has a detectable absorbance at 570 nm only when bound to an amine group. PCL mats with covalently immobilized laminin (attached and rinsed following the same procedure described in the Electrospun fiber modification section above) were soaked in 0.1 M ninhydrin in ethanol for 1 min and subsequently heated at 80 °C for 15 min, rinsed thoroughly with water, and dried for analysis, as described in the labeling protocol.[4,26] The surface-equivalent laminin concentration per mass of the fiber mat was calculated from a laminin/ninhydrin calibration curve, using a linear least-squares fit.

Total protein concentration was determined using a NanoOrange assay with a by difference approach. PCL mats were plasma treated, reacted with EDC/NHS, and then soaked in a laminin solution overnight. To remove unbound protein, the mats were sonicated 30 min in the working solution and rinsed with an aliquot of the working

solution (instead of the Tween rinse as done above due to the interference of the surfactant in the assay). Previous studies have demonstrated that 30 min of sonication is an equivalent means to remove physically adsorbed proteins. The protein soaking, sonication and rinse solutions were combined to serve as the final protein solution for spectrophotometric analysis. An aliquot of the protein solution was diluted into an equal volume of working solution to serve as the initial protein solution. The amount of protein covalently immobilized per mass of fiber mat was determined by taking the difference between the initial and final protein concentrations, and dividing by the weight of the fiber mat.

Culture of PC12 Cells. PC12 cells derived from the phenochromocytoma of the rat adrenal medulla were used to study the effect of protein concentration on neurite outgrowth. PC12 cells undergo neuron-like differentiation when treated with nerve growth factor and thus can serve as a model system to study neuronal differentiation and other properties. PC12 cells were cultured in RPMI 1640 medium supplemented with 10% heat-inactivated horse serum and 5% fetal bovine serum and 1% antibiotic/antimycotic "complete medium" here at 37 °C and 5% CO_2. Sterile fiber mats in 24-well plates were incubated in serum-free medium 2 h prior to seeding cells. For differentiation studies, cells were seeded at a density of 5000 cells/well in high-glucose DMEM with 1% horse serum, 0.5% calf serum, and 1% antibiotic/antimycotic "differentiation medium" here. After 24 h, 100 ng/mL NGF was added to the differentiation medium.

Neurite Outgrowth Study. After day 10 of seeding cells in differentiation medium supplemented with 100 ng/mL NGF, neurite outgrowth was characterized by staining actin filaments with phalloidin and analyzing with confocal laser scanning microscopy (CLSM). To prepare samples for CLSM, we rinsed the fiber scaffolds thoroughly with PBS and fixed in 4% paraformaldehyde in PBS for 20 min. Scaffolds were rinsed with PBS and cells were permeabilized with 0.2% Triton X-100 for 10 min. Nonspecific labeling was prevented by incubating samples in a blocking buffer composed of 3% bovine serum albumin (BSA) in PBS for 20 min. Samples were then immersed in rhodamine phalloidin (1:200) in blocking buffer for 1 h. Samples were rinsed thoroughly with PBS and kept in the dark at 4 °C until analysis.

Samples were imaged on a Zeiss LSM5 Pascal equipped with Epiplan-Neofluar lenses. The cells in the scaffolds were imaged with a 543 nm laser. A minimum of n = 5 random areas for each of 3 replicate fiber mat samples were imaged using the 10× and 20× objectives. Neurite length was measured using the Zeiss LSM software v 4.2.0.121.

Bioavailability Assay. The bioavailability of the PCL fibers with different concentrations of covalently attached laminin was evaluated using a fluorescent immunoassay. Samples were prepared and rinsed as previously described. Samples were then immersed in a blocking buffer (3% BSA in 10% donkey serum) to minimize nonspecific adsorption. Samples were then incubated in a polyclonal rabbit antilaminin antibody (1:200) in blocking buffer overnight at 4 °C. Subsequently, the samples were washed and incubated in AlexaFluor 488 donkey antirabbit secondary antibody (1:200) for 1 h at RT. The immunostained samples were imaged using CLSM microscopy on a Zeiss LSM5 Pascal. Detector gain and amplifier offset were kept constant for all samples to enable semiquantitative comparison. Unmodified PCL fiber controls, as well as controls to determine the nonspecific attachment of the secondary antibody and the autofluorescence of primary antibody and sample were also evaluated. A minimum of n = 5 random areas for each of 3 replicate fiber mat samples were imaged using the 2.5× objective with the refractive correlation set to 3. The mean and summed intensity were determined using the Zeiss LSM software v 4.2.0.121 histogram feature.

Statistics. All data are expressed as mean ± standard deviation (unless noted). One-way ANOVA with post hoc Tukey means comparison tests were conducted with a significance level of $p < 0.05$.

■ RESULTS

Electrospinning was used to fabricate PCL fibers with diameters ranging between 140 and 380 nm. In order to enhance the

hydrophilicity and biocompatibility of the fibers, fibers were air-plasma treated, and laminin protein was covalently immobilized using an EDC/NHS coupling reaction.[25] Figure 1 displays the
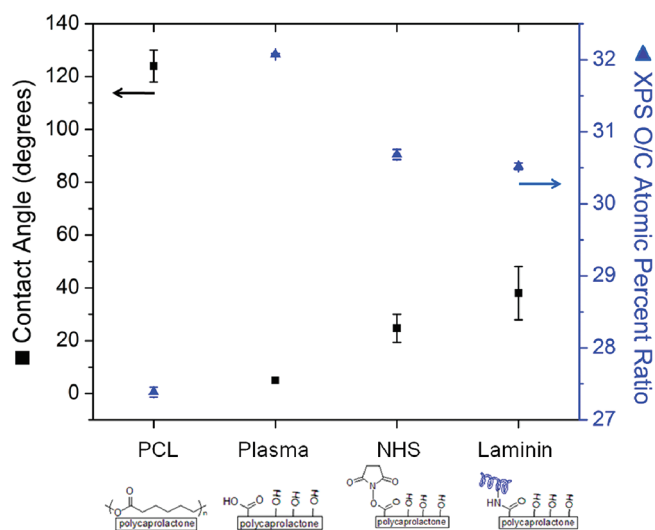

Figure 1. (Left vertical axis) Sessile-drop water contact angle of electrospun polycaprolactone (PCL) fiber mats with the following surface chemistries: (left to right) unmodified control (PCL), plasma-treated PCL (Plasma), plasma-treated PCL with covalently attached N-hydroxysuccinimide (NHS), plasma-treated PCL + NHS with covalently attached laminin (Laminin) (50 μg/mL protein solution concentration, 24 h). Error bars represent mean ± standard error of the mean, n = 15. (Right vertical axis) Atomic O/C ratios of native and modified polycaprolactone nanofibers as determined by X-ray photoelectron spectroscopy, mean ± standard deviation (n = 6). Error bars are occasionally smaller than data symbols.

water contact angle and XPS oxygen-to-carbon ratio (O/C) for each of the 4 steps in the modification procedure. After plasma treatment, the fiber mats showed a significant decrease in water contact angle from approximately 120 ± 6.1° to less than 5°, as shown in Figure 1 (left vertical axis). In addition, the atomic ratio of oxygen to carbon (O/C), as determined by XPS, increased after plasma treatment, (Figure 1, right vertical axis) as additional oxygen-containing species were incorporated into/onto the fibers. After NHS and protein attachment, the O/C ratio decreased slightly compared to the plasma-treated fiber ratio, due to the addition of carbon species from attached molecules. The contact angle increased to 40° after the attachment of protein (50 μg/mL protein solution concentration, 24 h), because additional hydrophobic carbon species were introduced onto the surface. Although we did not verify the contact angle of fiber mats reacted with different protein solution concentrations, we would expect a slight decrease in contact angle due to less protein and hence less carbon on the fiber surface.

Panels A and B in Figure 2 display the C 1s spectra for unmodified PCL and PCL with covalently attached laminin. An examination of the fitted C 1s components revealed a reduction in the amount of methyl/methylene carbon CH_3/CH_2 (68.8% to 51.1%), an increase in β carbon of the ester $*C-C=O$ (10.4% to 16.1%) and carbon bonded to the oxygen of the ester $C-O-C=O$ (10.6% to 12.4%), and a slight decrease in the carbon of the ester $*C-O-C=O$ (10.4% to 8.2%) for the plasma-treated PCL fibers with covalently attached laminin in comparison to native PCL fibers.
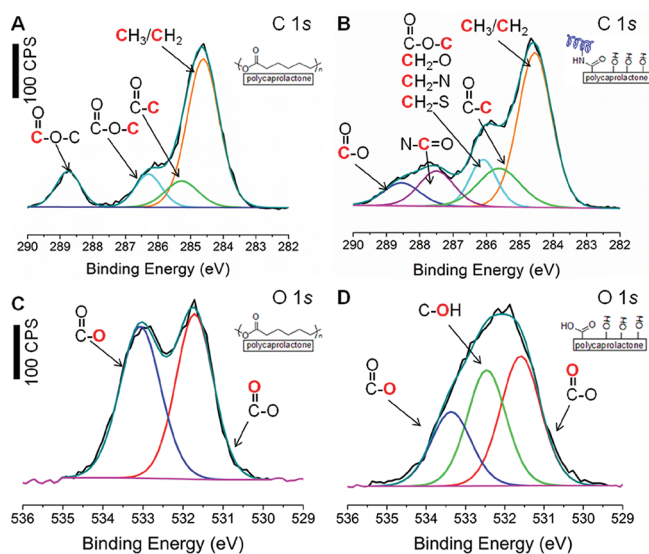
Figure 2. High-resolution X-ray photoelectron spectra of electrospun polycaprolactone (PCL) fibers. (A) XPS C 1s of unmodified PCL fibers, (B) XPS C 1s of plasma-treated PCL fibers with covalently attached laminin, (C) XPS O 1s of unmodified PCL fibers, (D) XPS O 1s of plasma-treated PCL fibers.

The XPS data confirmed the addition of oxygen-containing species by the plasma treatment, including hydroxyl and carboxylic acids, which was also verified by contact angle measurements. In addition, a fifth component appeared (amide, 12.1%) at 287.5 eV, and the nitrogen atomic percentage increased from 0 to 7.2 ± 0.8 at % for the 50 μg/mL laminin solution (Figure 2B). Panels C and D in Figure 2 display the unmodified PCL fiber and plasma-treated PCL fiber O 1s XPS spectra. The native PCL fiber spectrum consisted of the

carbonyl oxygen O−C=**O*** and ester oxygen ***O**−C=O components in a near 50:50 ratio. After plasma treatment, the O 1s spectrum contained a third component for hydroxyl C−**O***−H (35.5%), with the carbonyl O−C=**O*** and ester ***O**−C=O oxygen compositions being reduced to 41.0 and 23.5%, respectively.

After preparation of the PCL scaffolds and confirmation of protein attachment, methods to control the amount of protein attached to the fiber surface were explored using two approaches for which results are displayed in Figure 3—varying reaction time at constant protein concentration and varying protein solution concentration at fixed time. In the first approach, the fiber mat was immersed in either a 25 or 50 μg/mL laminin solution for time periods between 1 min and 100 h. As can be seen in Figure 3A and its insets, protein−surface reaction occurred rapidly for the first hour as evidenced by the XPS nitrogen-to-carbon (N/C) atomic percent ratio, slowed for a few hours, and then increased again from 4 to 24 h. We surmise that the first plateau is indicative of the completion of one protein "monolayer," whereas the second slow rise at longer reaction times is indicative of physisorption of subsequent protein layers onto the first protein "monolayer." Thus we are using the term "monolayer" here in the same sense as its conventional definition, i.e., the coverage at which additional protein adsorption would have to occur on proteins, not on fibers. Proteins in the first monolayer are assumed to be covalently attached and fully covering the fiber surface. Additional protein coverage, forming the second and subsequent monolayers defined by us as "multilayer" coverage, means that the proteins are not covalently bound, but rather physically adsorbed to the fiber surface. Excessively high protein concentration or long reaction times can lead to the multilayer coverage state.
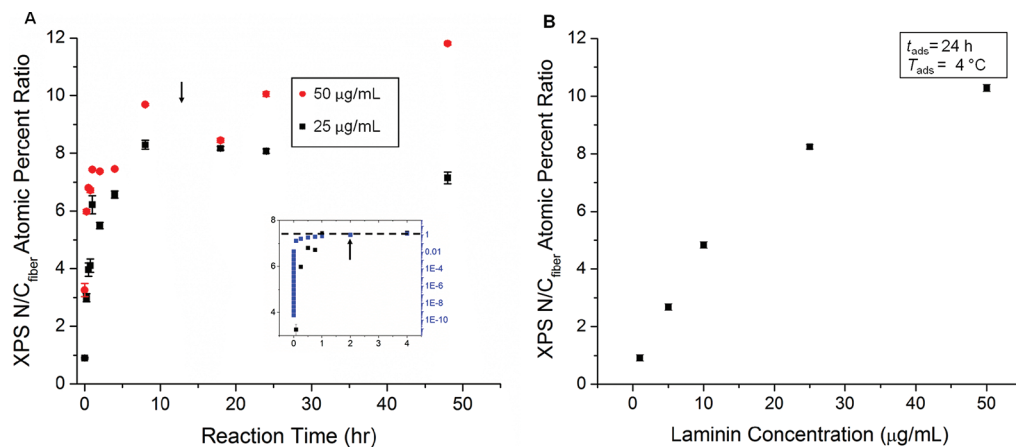

Figure 3. XPS nitrogen-to-carbon atomic percent ratios of polycaprolactone electrospun nanofibers. The XPS carbon contribution from the protein was subtracted based on the known nitrogen-to-carbon stoichiometry in the protein in order to normalize the N XPS protein signal to the C XPS signal from the fibers only. This provides a zero-order correction to the N-to-C ratio that considers only carbon in the fibers and not C in the protein. However, attenuation effects will reduce the XPS C signal further, an effect that we did not attempt to account for here. (A) Fibers were plasma-treated, reacted with *N*-hydroxysuccinimide, and soaked in a 25 or 50 μg/mL laminin solution for various time periods to effect the covalent attachment of the protein to the fiber surface. The arrow denotes the 24 h time-point, calculated to be the point when one protein monolayer coverage occurs, based on the diffusion coefficient for laminin in free solution. Inset displays 0 to 4 h reaction region with the same left axis label as the main plot, and protein coverage (fractional protein monolayers), determined from the diffusion coefficient for laminin at 2 h reaction time (right axis, blue squares). The arrow and the dashed line denote the 2 h time-point, calculated to be the approximate point when one protein monolayer coverage occurs, on the basis of the XPS data. (B) Fibers were plasma treated, reacted with *N*-hydroxysuccinimide and soaked in laminin solutions with concentrations from 1 to 50 μg/mL for 24 h at 4 °C to effect the covalent attachment of the protein to the fiber surface. Error bars (mean ± standard deviation, $n = 6$) are generally smaller than data symbols.

Because it was difficult to precisely control reaction time, especially at short times, a second method was explored in which the reaction time was fixed at 24 h and the protein concentration was varied. For the latter method, five protein concentrations were selected between 1 and 50 μg/mL. As can be seen in Figure 3B, a strong correlation between protein concentration and XPS N/C atomic percent ratio was observed. (The form of the data for both approaches resembled a Langmuir-like adsorption process, even though not all Langmuirian assumptions are met.)

Because the covalent attachment of protein molecules depends on diffusion-limited kinetics, we modeled the diffusion of laminin in solution to determine the maximum number of protein molecules adsorbed as a function of time for the first method of protein attachment (time-based). The theoretical surface concentration n was calculated using the following equation:

$$n = 2C_o(Dt/\pi)^{1/2} \tag{1}$$

where n = mass of protein molecules/fiber area (g/cm^2), C_o = solution protein concentration (g/mL), D = diffusion coefficient (cm^2/s), and t = time (s).[27] This model assumes the average radius of the laminin protein to be 3 nm, which compares well with values determined by Atomic Force Microscopy (2.3 nm).[28] Fitting of the plot of protein molecules/fiber area versus time revealed monolayer coverage, and hence the onset of physical adsorption at 24 h for a 50 μg/mL protein solution concentration. Surface protein coverage determined by XPS and the laminin diffusion model was calculated by dividing the XPS N/C ratio for each protein solution concentration (shown in Figure 3B) by the XPS N/C ratio at the 24 h time-point (shown by arrow in Figure 3A). Because the XPS time-based study indicated that a protein monolayer formed at approximately 2 h rather than the 24 h predicted by the model, we used this time-point to calculate the diffusion coefficient of laminin through the nanofiber mat (1 × 10^{-16} cm^2/s). Fractional protein monolayers were also calculated using the XPS N/C ratio at the 2 h time-point as described above (shown by the arrow in the Figure 3A inset). The results, representing fractional protein monolayer coverage, are displayed in Table 1. Because good control over protein incorporated onto the surface of the fiber mats was achieved using the second method (concentration-based), the rest of the paper presents results using this method.

Because XPS probes only the top few nanometers of the surface, estimations of total protein in the 3D fiber mat could only be assumed by extrapolation of results derived from the surface of the outermost fibers of the mat. To quantify the total amount of protein covalently immobilized onto the fiber mats and understand trends in the surface and total protein coverage, were examined two different fluorescence-based assays. In the first method, the total amount of protein was quantified using the NanoOrange protein-quantification reagent. This reagent is designed to measure the concentration of proteins in solution, so a "by-difference" approach was utilized in which the total amount of protein attached to the fiber mat was determined by taking the difference between the initial protein solution concentration and postreaction protein solution concentration, after accounting for dilution. The concentration of reacted laminin on the fiber mat was determined from a calibration curve for the protein in solution. The fiber mats were rinsed in a fixed volume of the NanoOrange protein-quantification

Table 1. Laminin Concentration and Protein Coverage on Polycaprolactone Electrospun Fibers As Determined by X-ray Photoelectron and Ultraviolet–Visible Spectroscopy

solution LN concn (μg/mL)	LN[a]/ COOH[b]	calcd LN monolayers[c]	calcd LN monolayers[d]
1	1.99	0.13	0.09
5	2.94	0.36	0.27
10	6.48	0.66	0.48
25	14.22	1.12	0.82
50	18.75	1.39	1.02

[a]On the basis of a ninhydrin assay for laminin; laminin concentrations are the solution-phase equivalent concentrations normalized to fiber mat mass (μM/mg fiber mat). [b]On the basis of 5-(aminoacetamido) fluorescein assay for surface COOH groups; COOH concentrations are the solution-phase equivalent concentrations normalized to fiber mat mass (μM/mg fiber mat). [c]On the basis of the XPS N/C (24 h) at each LN solution concentration, normalized to the one-monolayer-coverage value of the XPS N/C ratio at 2 h determined from a time-based adsorption experiment. [d]On the basis of the XPS N/C (24 h) at each LN solution concentration, normalized to the one-monolayer-coverage value of the XPS N/C ratio at 24 h determined from a time-based adsorption experiment.

reagent. This "by-difference" assay relies on the fact that the fiber mat presents a significant surface area with which the protein can react. The assay would probably not be useful for planar, low-surface-area samples.

Figure 4 displays the difference concentration, representing the amount of protein reacted with the fiber mat, normalized to the mass of the fiber mat. A linear trend was observed for total protein (normalized to fiber mass) vs solution protein concentration for solution concentrations up to 40 μg/mL. At concentrations above 40 μg/mL, the linear trend changed to a steeper dependence on solution protein concentration, most likely due to multilayer formation. (The 100 μg/mL data point (0.059 ± 0.0047 μM/mg fiber mat, n = 3 (not shown)) further confirmed the trend).

In the second fluorescence-based method, the antibody bioavailability of the protein was determined and correlated to the amount of protein in its active antilaminin-binding form. The bioavailability of laminin (normalized to the XPS N/C ratio or total protein determined from the NanoOrange assay) was highest for the fiber mats reacted with the 1–2 μg/mL protein solutions, and then decreased rapidly with increasing protein soaking concentration. The change in bioavailability reached a plateau, such that for the fiber mats reacted with greater than 10 μg/mL laminin soaking solution, the antibody bioavailability change was insignificant. A cell culture assay was developed to probe the cellular bioavailability of the fiber mats, which is discussed in the last part of this section.

As discussed previously, XPS provides information about surface atomic compositions, but does not reveal quantitative compositional information about the 3D fiber mat. Different diffusion rates of reactants and penetration depth of the plasma can potentially cause the total functional group composition of the mat to vary as a function of depth. To quantitatively evaluate the total carboxylic acid content of the fiber mats after plasma treatment, we developed an assay with 5-(amino-acetamido) fluorescein dye. The dye contains free amines that can form covalent bonds with carboxylic acids in the presence of coupling agents such as EDC. Unreacted and physically adsorbed dye was removed, and the absorbance of the covalently bound dye in the full fiber mat was analyzed with
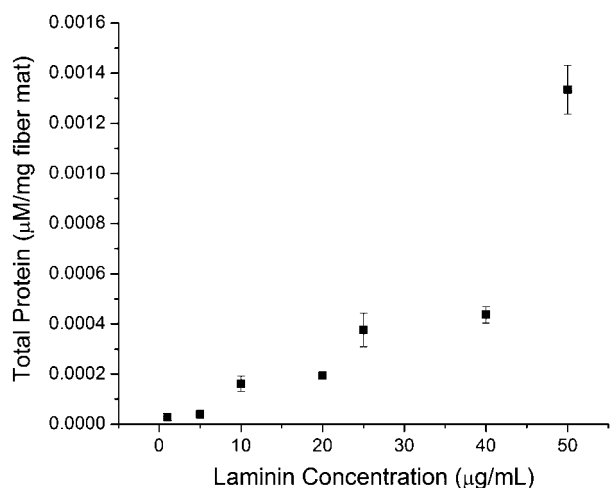
2078

dx.doi.org/10.1021/am300045y | ACS Appl. Mater. Interfaces 2012, 4, 2074–2081

Figure 4. Total protein on the fibers in the polycaprolactone electrospun 3D fiber mat as determined by a fluorescence assay. Fibers were plasma treated, reacted with *N*-hydroxysuccinimide, and soaked in laminin solutions with concentrations from 1 to 50 μg/mL for 24 h at 4 °C to effect the covalent attachment of the protein to the fiber surface. In this difference assay, to remove and then label unbound protein, the mats were sonicated and rinsed with the fluorescent labeling solution. The protein soaking, sonication, and rinse solutions were added together to serve as the final "removed protein" fluorescence samples. An aliquot of the initial unreacted protein solution was diluted in an equal volume of fluorescent labeling solution to serve as the sample for the initial protein concentration. The surface-equivalent concentration of protein covalently immobilized on the fibers of the mat was determined by the difference between the initial and final protein concentrations, and then normalized to the mass of fiber mat. Error bars represent mean $\pm$ standard deviation ($n = 3$), and are occasionally smaller than data symbols.

UV−vis. Results are shown in Figure 5. The concentration of 5-(aminoacetamido) fluorescein dye, which has 1:1 binding stoichiometry with carboxylic acids, was determined from a calibration plot for the dye in solution. As evidenced by the relative peak areas, unmodified PCL had the lowest observed concentration of carboxylic acids (1.62 ± 0.6 nM/mg fiber mat, $n = 3$); the signal most likely arising from residual physisorbed dye molecules. Unmodified PCL that was soaked in EDC/NHS had a similar concentration (2.79 ± 1.6 nM/mg fiber mat, $n = 4$). Plasma-treated PCL reacted with EDC/NHS had the highest concentration (177 ± 37 nM/mg fiber mat, $n = 3$), as expected. Stated another way, the plasma-treated fibers reacted with EDC/NHS exhibited greater than 60 times more reactive carboxylic groups per unit area than the control mats.

The total amount of laminin was also determined using UV−vis spectroscopy and a modified procedure as described above.[4,26] For these experiments, fiber mats were reacted with ninhydrin dye, rinsed and dried for analysis. The ninhydrin dye absorbs at 570 nm only when covalently bound to an amine, providing a useful tag for protein quantification. The protein concentration was calculated from a calibration of laminin reacted with ninhydrin in ethanol. Using the highest concentration of carboxylic acid binding sites observed (background corrected), the amount of carboxylic acid groups on the fiber surface consumed in the reaction with the protein was determined by dividing the laminin concentration (observed at each protein solution concentration) by the maximum carboxylic acid concentration (determined from the
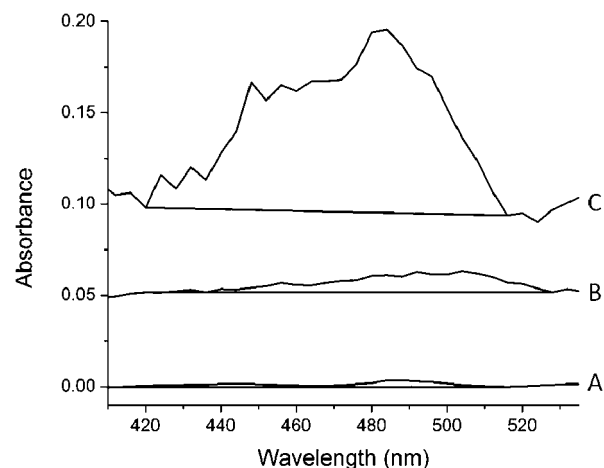

Figure 5. Assay to determine available carboxylic acid groups on electrospun PCL fibers. Unmodified PCL mats and unmodified and plasma-treated PCL mats reacted with EDC/NHS were soaked overnight in 0.1 mM 5-(aminoacetamido) fluorescein solution in PBS at RT with gentle shaking. The mats were then rinsed thoroughly and dried for analysis. Equivalent concentration of surface carboxylic acid per mass of fiber mat (mM/mg fiber mat) was calculated from a 5-(aminoacetamido) fluorescein calibration curve. PCL fibers with covalently attached 5-(aminoacetamido) fluorescein dye, containing a free amine, was used to react with and label carboxylic acid groups on: (A) unmodified control PCL fibers, (B) unmodified control PCL fibers reacted with *N*-hydroxysuccinimide, (C) plasma-treated PCL fibers reacted with *N*-hydroxysuccinimide. Baselines shown were used in the assay quantification. Spectra are offset on absorbance axis for clarity.

plasma-treated samples in the fluorescein assay). As can be seen in Table 1, 1:1 laminin to carboxylic binding stoichiometry occurred at less than the 1 μg/mL laminin reaction concentration. Approximately 14 laminin molecules were bound to 1 carboxylic group for one protein monolayer, as determined by XPS using the 2 h time-point, suggesting the UV−vis model predicted faster protein-adsorption rates compared to the XPS model. Although not necessarily equivalent to monolayer coverage, because a single laminin molecule can form bonds to many surface carboxylic sites, these stoichiometry results suggest that there were physically adsorbed laminin proteins on fiber mats reacted in protein solutions at and above the 1 μg/mL concentration.

The neurite outgrowth of neuron-like PC12 cells, which differentiate like neurons when treated with nerve growth factor and respond to ECM proteins through integrin surface-receptors, were used to assess the bioavailability of the protein-modified fiber scaffolds (in addition to the bioavailability immunoassay discussed earlier). The neurite outgrowth was found to be highly dependent on the amount of protein on the fibers in the fiber mat. Figure 6A displays the neurite lengths for protein soaking solution concentrations ranging between 1 and 50 μg/mL. The difference in neurite length was found to be statistically significant for mats formed from each protein solution concentration except between the 10 and 25 μg/mL concentration levels. Figure 6B displays representative CLSM images of PC12 cells grown on mats soaked in the 1 and 50 μg/mL protein solutions. As can be seen, the lengths of the neurites are significantly longer on the 50 μg/mL samples compared to the 1 μg/mL samples. The number of neurites per cell was calculated and ranged between 0.6 for the 1 μg/mL samples to 1.7 for the 50 μg/mL. Yet, there was no significant
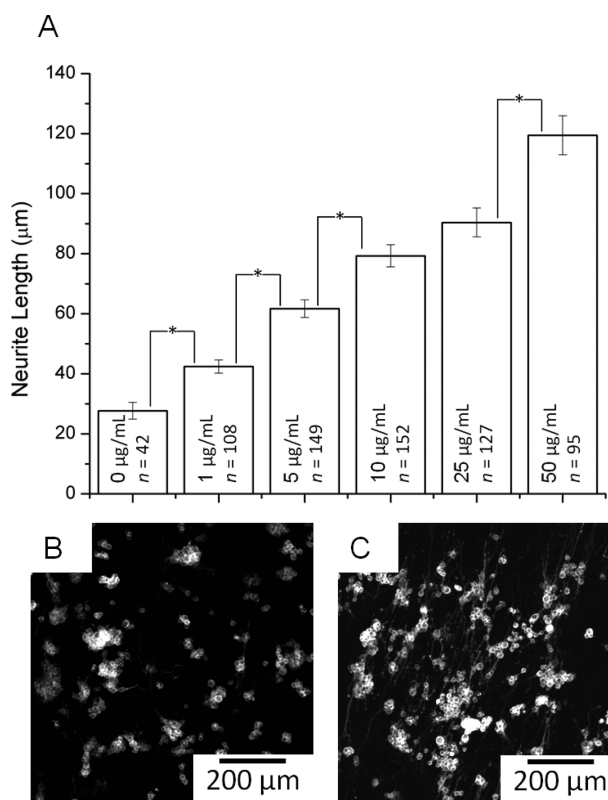
A

B   C

Figure 6. (A) Outgrowth of neuron-like PC12 cells cultured on oriented polycaprolactone electrospun fibers with covalently attached laminin. Fibers were plasma treated, reacted with *N*-hydroxysuccinimide, and soaked in laminin solutions with concentrations from 1 to 50 μg/mL for 24 h at 4 °C to effect the covalent attachment of the protein to the fiber surface. Data are expressed as mean ± standard error of the mean (*$p < 0.05$). (B, C) Representative examples of confocal laser scanning microscopy images of PC12 cells on plasma-treated electrospun polycaprolactone fibers with covalently attached *N*-hydroxysuccinimide soaked in (B) 1 μg/mL laminin solution for 24 h, and (C) 50 μg/mL laminin solution for 24 h. Actin components in the neurites were stained by immersion in rhodamine phalloidin (1:200) in blocking buffer for 1 h.

difference between the number of neurites for cells grown on mats formed by soaking in solutions of laminin ranging between 10 and 50 μg/mL.

■ DISCUSSION

Modern bioengineering teaches us that the attachment of proteins to tissue engineering scaffolds can modify and improve the biological response to that material. However, methods to control the amount of protein incorporated into the scaffold, techniques for protein quantification, and the effect of protein concentration on cellular processes on electrospun scaffolds have been little explored. Here we have examined surface and total protein and functional group concentrations, to help provide insight into the rates of protein adsorption, surface coverage, and their effect on cell behavior.

A comparison of protein monolayer coverage, as approximated by the XPS 2 h time-point and as calculated from the diffusion model for laminin (24 h time-point), is presented in Table 1. Calculations from the 2 h time-point predicted a saturated covalent protein monolayer to form for mats reacted in the 25 μg/mL protein solution (24 h), whereas the diffusion model predicted this to occur at the higher protein solution

concentration (50 μg/mL, 24 h). Given the assumptions in the diffusion model, this is fairly good agreement. The change in slope from linear to nonlinear or submonolayer to multilayer protein coverage for the NanoOrange assay occurred between these two concentrations (between 40 and 50 μg/mL), and thus agreed well with the XPS data. The protein coverage predicted by the UV–vis model was 8–15 times higher than both the XPS or NanoOrange fluorescence models. This may be due to the slower reaction rate of the ninhydrin dye with the laminin in solution, and thus use of an inaccurate calibration to determine the laminin concentration on the surface of the fibers in the solid fiber mats. There could also be error in the calculation of the carboxylic acid concentration used as the denominator in the protein monolayer equation (LN/COOH). As discussed above, the XPS 24 h time-point was determined by fitting the function of the diffusion model for laminin in free solution. Although diffusion rates were much slower for our fibrous system, when compared to the laminin diffusion model, monolayer formation actually occurred faster, possibly because of the high surface area of our fiber mats compared to the planar surface assumed in the model.

In this work, we have focused on determining protein concentration and coverage, which are both important factors to consider when designing tissue scaffolds. In addition, the protein conformation can also play a critical role in the functionality of the scaffolds, although it has not been systemically studied to our knowledge. From the UV–vis data, we calculated the theoretical laminin-to-carboxylic binding ratio at lower protein-reaction concentrations. From this data, we inferred fractional protein monolayer coverage based on 1:1 laminin-to-carboxylic acid binding stoichiometry. Because the protein can form multiple covalent bonds to the fiber surface, which likely occurred for mats reacted with low protein solution concentrations, we can only surmise that the average conformation of the protein changed on our fiber surfaces as a function of protein coverage. In addition, the protein coverage is important to consider since the bioactivity of the protein-functionalized surface may change depending on the type of protein immobilized.[29] Protein coverage greater than a monolayer is indicative of the presence of physically adsorbed proteins, which could have important implications for certain applications. Based on the protein reaction graphs in Figure 3, and the data in Table 1, it is possible to control the surface coverage of protein based on reaction times or protein solution concentrations. Because the focus of this study was to characterize, rather than control, protein coverage, and we found an improvement in PC12 cell differentiation with increased protein concentration (including multilayer coverage), we did not explore the formation of scaffolds with solely monolayer protein coverage. In previous work, laminin was found to be approximately equally active in promoting neurite outgrowth in both its covalent and physically adsorbed forms, but other biomolecules may exhibit more conformation-dependent behavior.[25,30,31]

The antibody bioavailability assay showed no significant difference between the amount of laminin in its active antilaminin binding form between 10 and 50 μg/mL, although additional surface protein did apparently provide more binding domains, resulting in enhanced neurite outgrowth rates with increasing protein coverage. The laminin used in these studies was ca. 95% pure, and thus contained some impurities, including collagen type IV and heparan sulfate proteoglycan, which could have contributed to the increased neurite

2080

dx.doi.org/10.1021/am300045y | *ACS Appl. Mater. Interfaces* 2012, 4, 2074–2081

outgrowth observed. The maximum concentrations of each of the two main impurities (1.4 μg/mL) was less than the amounts determined to have an effect on neurite outgrowth as determined by Lein et al. and Lesma et al.[32,33] In addition, B. Li et al., as well as G. Li et al., have observed dose-dependent responses of PC12 and DRG neuron cells, respectively, to mouse laminin of the same purity.[34,35]

CONCLUSIONS

Electrospun PCL nanofibers were fabricated and functionalized with covalently attached laminin to test for improvements in bioactivity. The amount of protein on the surface of the fibers in the fiber mat was controlled by varying the reaction time and protein solution concentration. Several methods to compare the concentration of protein, both at the mat surface and in the 3D mat, were evaluated. Normalized XPS results showed a nearly linear increase in protein coverage with concentration until a monolayer was formed. Fluorescence and UV–vis assays were explored to quantify the total protein and functional groups in the fiber mat. For the aforementioned assays, total protein coverage increased linearly for the lower solution concentrations, and increased more rapidly for solution concentrations above 40 μg/mL due to multilayer formation. Quantification of the total carboxylic acid content, introduced from the plasma treatment of the fiber mat, by a fluorescein assay, along with calculation of laminin concentrations from a ninhydrin assay, enabled the calculation of the carboxylic reaction site consumption at different protein solution concentrations. Although protein conformational changes could only be inferred from these experiments, further studies on protein conformation at different surface coverages would aid in the understanding of these systems. To the best of our knowledge, control of protein conformation has not been achieved on fibers.

Although the antibody bioavailability of laminin was not greatly affected above about 10 μg/mL protein concentration, the neurite outgrowth of PC12 cells exhibited a strong positive correlation with significantly longer neurites observed on the fiber mats containing higher protein concentrations. Thus, the ability to control and quantify protein coverage in electrospun fibers mats has been achieved. The uncontrolled variable, that of protein conformation as a function of coverage, is likely to be critical in the design of tissue engineering scaffolds.

AUTHOR INFORMATION

Corresponding Author
*E-mail: nicole.e.zander.civ@mail.mil.

Notes
The authors declare no competing financial interest.

REFERENCES

(1) Shi, J.; Wang, L.; Zhang, F.; Li, H.; Lei, L.; Liu, L.; Chen, Y. *ACS Appl. Mater. Interfaces* **2010**, *2*, 1025−1030.
(2) Ratner, B. D.; *Biomaterials Science*; Hoffman, A. S., Schoen, F. S., Lemons, J. E., Eds.; Elsevier Science: San Diego, 1996.
(3) Cao, H. Q.; Liu, T.; Chew, S. Y. *Adv. Drug Delivery Rev.* **2009**, *61*, 1055−1064.
(4) Mattanavee, W.; Suwantong, O.; Puthong, S.; Bunaprasert, T.; Hoven, V. P.; Supaphol, P. *ACS Appl. Mater. Interfaces* **2009**, *1*, 1076−1085.
(5) Nisbet, D. R.; Yu, L. M. Y.; Zahir, T.; Forsythe, J. S.; Shoichet, M. S. *J. Biomater. Sci., Polym. Ed.* **2008**, *19*, 623−634.
(6) Yoo, H. S.; Kim, T. G.; Park, T. G. *Adv. Drug Delivery Rev.* **2009**, *61*, 1033−1042.
(7) Li, M. Y.; Guo, Y.; Wei, Y.; MacDiarmid, A. G.; Lelkes, P. I. *Biomaterials* **2006**, *27*, 2705−2715.
(8) Ghasemi-Mobarakeh, L.; Prabhakaran, M. P.; Morshed, M.; Nasr-Esfahani, M. H.; Ramakrishna, S. *Biomaterials* **2008**, *29*, 4532−4539.
(9) Li, M.; Mondrinos, M. J.; Chen, X.; Gandhi, M. R.; Ko, F. K.; Lelkes, P. I. *J. Biomed. Mater. Res. A* **2006**, *79A*, 963−973.
(10) Neal, R. A.; McClugage, S. G.; Link, M .C.; Sefcik, L. S.; Ogle, R. C.; Botchwey, E. A. *Tissue Eng. Part C* **2009**, *15*, 11−21.
(11) Discher, D. E.; Mooney, D. J.; Zandstra, P. W. *Science* **2009**, *324*, 1673−1677.
(12) Li, W.; Laurencin, C. T.; Caterson, E. J.; Taun, R. S.; Ko, F. K. *J. Biomed. Mater. Res.* **2002**, *60* (4), 613−621.
(13) Lutolf, M. P.; Hubbell, J. A. *Nat. Biotechnol.* **2005**, *23* (1), 47−55.
(14) Greiner, A.; Wendorff, J. H. *Angew. Chem., Int. Ed.* **2007**, *46*, 5670−5703.
(15) Li, D.; Xia, Y. N. *Adv. Mater.* **2004**, *16*, 1151−1170.
(16) Huang, Z. M.; Zhang, Y. Z.; Kotaki, M.; Ramakrishna, S. *Compos. Sci. Technol.* **2003**, *63*, 2223−2253.
(17) Xie, J. W.; MacEwan, M. R.; Li, X. R.; Sakiyama-Elbert, S. E.; Xia, Y. N. *ACS Nano* **2009**, *3*, 1151−1159.
(18) Yang, F.; Murugan, R.; Wang, S.; Ramakrishna, S. *Biomaterials* **2005**, *26*, 2603−2610.
(19) Grafahrend, D.; Calvet, J. L.; Klinkhammer, K.; Salber, J.; Dalton, P. D.; Möller, M.; Klee, D. *Biotechnol. Bioeng.* **2008**, *101*, 609−621.
(20) Lee, Y.; Arinzeh, T. L. *Polymers* **2011**, *3*, 413−426.
(21) Sangsanoh, P.; Waleetorncheepsawat, S.; Suwantong, O.; Wutticharoenmongkol, P.; Weeranantanapan, O.; Chuenjitbuntaworn, B.; Cheepsunthorn, P.; Pavasant, P.; Supaphol, P. *Biomacromolecules* **2007**, *8*, 1587−1594.
(22) Straley, K. S.; Heilshorn, S. C. *Soft Matter* **2008**, *5*, 114−124.
(23) Dertinger, S. K. W.; Jiang, X.; Li, Z.; Murthy, V. N.; Whitesides, G. M. *Proc. Natl. Acad. Sci. U.S.A.* **2002**, *99*, 12542−12547.
(24) Adams, D. N.; Kao, E. Y.; Hypolite, C. L.; Distefano, M. D.; Hu, W.; Letourneau, P. C. *J. Neurobiol.* **2005**, *62*, 134−147.
(25) Koh, H. S.; Yong, T.; Chan, C. K.; Ramakrishna, S. *Biomaterials* **2008**, *29*, 3574−3782.
(26) Bramfeldt, H.; Vermette, P. *J. Biomed. Mater. Res. A* **2009**, *88A*, 520−530.
(27) Andrade, J. D., *Surface and Interfacial Aspects of Biomedical Polymers*; Plenum Press: New York, 1985; Vol. 2, p 29−31.
(28) Chen, C. H.; Clegg, D. O.; Hansma, H. G. *Biochemistry* **1998**, *37*, 8262−8267.
(29) Williams, R. A; Blanch, H. W. *Biosens. Bioelectron.* **1994**, *9*, 159−167.
(30) Polini, A.; Pagliara, S.; Stabile, R.; Netti, G. S.; Roca, L.; Prattichizzo, C.; Gesualdo, L.; Cingolani, R.; Pisignano, D. *Soft Matter* **2010**, *6*, 1668−1674.
(31) Zander, N.; Orlicki, J.; Rawlett, A.; Beebe, T. *Biointerphases* **2010**, *5* (4), 149−158.
(32) Lein, P. J.; Higgins, D.; Turner, D. C.; Flier, L. A.; Terranova, V. P. *J. Cell. Biol.* **1991**, *113* (2), 417−428.
(33) Lesma, E.; Di Giulio, A. M.; Ferro, L.; Prino, G.; Gorio, A. *J. Neurosci. Res.* **1996**, *46*, 565−571.
(34) Li, B.; Ma, Y.; Wang, S.; Moran, P. M. *Biomaterials* **2005**, *26*, 1487−1495.
(35) Li, G. N.; Liu, J.; Hoffman-Kim, D. *Ann. Biomed. Eng.* **2008**, *36* (6), 889−904.